Ultrasonics Sonochemistry 94 (2023) 106314

Contents lists available at ScienceDirect

Ultrasonics Sonochemistry

journal homepage: www.elsevier.com/locate/ultson

Emulsions stabilised by casein and hyaluronic acid: Effects of high intensity ultrasound on the stability and vitamin E digestive characteristics

Ningzhe Wang [a], Jianjun Cheng [a], Yunqing Jiang [a], Yao Meng [a], Kaida Zhang [a], Qingfeng Ban [a,b,c,*], Xibo Wang [a,*]

[a] College of Food Science, Northeast Agricultural University, Harbin 150030, China
[b] Department of Endocrinology, Affiliated Hospital of Jining Medical University, Jining 272007, China
[c] Moxibustion College, Shandong University of Traditional Chinese Medicine, Jinan 250355, China

ARTICLE INFO

Keywords:
Casein
Hyaluronic acid
High-intensity ultrasound treatment
Emulsion stability
Vitamin E
Delivery carrier

ABSTRACT

This study aimed to prepare an emulsion stabilised by an ultrasound-treated casein (CAS)-hyaluronic acid (HA) complex and to protect vitamin E during in *vitro* digestion. It was found that high-intensity ultrasound (HIU) treatment significantly changed the hydrogen bonding, electrostatic interaction and hydrophobic interaction between CAS and HA, reduced the particle size of the CAS-HA complex, increased the intermolecular electrostatic repulsion, and thus significantly improved the emulsifying properties of the CAS-HA complex. Meanwhile, the creaming index (CI) and confocal laser scanning microscopy images showed that the stability of the CAS-HA-stabilised emulsion was the best when treated at 150 W for 10 min, which could be attributed to the enhanced adsorption capacity of the CAS-HA complex at the oil–water interface and the viscosity of the formed emulsion. In *vitro* digestion experiments revealed that the emulsion stabilised by the ultrasound-treated CAS-HA complex had a good protective effect on vitamin E. This study is significant for the development of emulsions for the delivery of lipophilic nutrients.

1. Introduction

Recently, information on the delivery of functional lipophilic nutrients to improve human health has attracted increasing attention. Vitamin E, a lipophilic bioactive substance, can prevent cell aging and reduce the risk of dementia, cancer, cardiovascular disease, and other illnesses [1]. However, the chemical stability of vitamin E is weak and is vulnerable to environmental influences, leading to its low bioavailability [2]. Various delivery systems have been reported to act as delivery carriers of lipophilic bioactive substances, including nanoemulsions, emulsion gels, liposomes, and microcapsules [3]. To improve the bioavailability of vitamin E, it is crucial to construct an appropriate delivery carrier for effective protection, delivery and release. It has been observed that the bioavailability of lipophilic bioactive substances can be improved with many emulsion-based delivery carriers [4]. Consequently, encapsulating vitamin E in an emulsion could be a potential way to improve its stability and bioavailability.

Casein (CAS) is recognised as a renewable, abundant, safe, highly functionality, and nutritionally valuable protein, consisting of α_{s1}-, α_{s2}-, β-, and κ-casein [5]. Casein-based emulsions have also been recognized as an useful delivery system mainly due to its low biological toxicity, high biocompatibility, and emulsifying properties [6]. However, traditional chemical processes, such as acidification and solidification, destroy the natural condition of casein micelles, leading to their poor emulsifying properties [7]. Especially under the highly acidic conditions, CAS is prone to aggregation and precipitation and is susceptible to hydrolysis by pepsin in the stomach, which limits its application in the delivery of biologically active substances [6]. Consequently, the widespread use of CAS as a suitable carrier for lipophilic bioactive substances poses a considerable technical challenge.

To enhance the stability of casein-based emulsions in the gastrointestinal tract, an effective strategy is to combine them with other colloidal components to create more robust and stable composite interfaces. Recently, polysaccharides have been found to enhance the stability of protein-based emulsions during storage and under simulated gastrointestinal conditions, affecting the absorption efficiency of the emulsion-loaded drugs and nutrients in the gastrointestinal tract [4]. Complexes formed by CAS and polysaccharides, such as xanthan gum

* Corresponding authors at: College of Food Science, Northeast Agricultural University, Harbin, 150030, China (Q. Ban).
E-mail addresses: qfban@neau.edu.cn (Q. Ban), wangxibo@neau.edu.cn (X. Wang).

https://doi.org/10.1016/j.ultsonch.2023.106314
Received 17 November 2022; Received in revised form 19 January 2023; Accepted 24 January 2023
Available online 28 January 2023

[8], pectin [9], and flaxseed gum [10] have been reported to be used as emulsifiers to create more stable emulsions. In addition, various lipophilic bioactive substances such as curcumin [4], lycopene [11], and lutein [12] have been encapsulated by casein-polysaccharide-stabilised emulsions. As previously mentioned, the combination with polysaccharides enables the casein-based emulsion to have greater stability and the ability to protect the gastrointestinal tract. Hyaluronic acid (HA), consisting of repeating *N*-acetyl-$_D$-glucosamine and $_D$-glucuronic acid disaccharide units, is widely distributed in the connective tissues of animals [13]. HA has received approval in many countries as a food ingredient [14]. It can combine with proteins through specific interactions and participate in many biological functions, such as anti-aging, anti-inflammation, angiogenesis, embryonic development, and free radical scavenging [15,16]. Previous studies have shown that the zein-HA binary complex as a delivery vehicle can protect quercetagetin in gastrointestinal digestion [13]. In addition, liquid lipid nanocapsules composed of bovine serum albumin and HA, improved the biological accessibility of curcumin [15]. Zhong et al. [17] used the whey protein isolate-HA complex to load curcumin and studied the effect of ionic strength on this delivery system. These studies suggest that HA has potential as a delivery carrier. Currently, the emulsion stabilised by the CAS-HA complex has not been reported for lipophilic bioactive substance encapsulation.

Although the protein-polysaccharide complex has the potential to improve the functional properties of a single substance, its particle size will increase and the bond will become unstable [18]. Therefore, a suitable modification method must be used to further enhance the functional properties and stability of the complexes. High-intensity ultrasound (HIU) treatment has many advantages such as simple, high efficiency, and energy saving [19]. Currently, HIU treatment has been shown to be useful in altering the structure of protein-polysaccharide complexes to provide more desirable emulsifying properties [18]. According to the report by Albano and Nicoletti [20], HIU treatment changed the viscosity of the solutions and reduced the size of the soluble pectin-whey protein concentrate complexes, leading to the improved emulsifying stability. In a subsequent study by Ma et al. [21], HIU treatment improved the zeta potential and surface hydrophobicity of electrostatic citrus pectin (CP)-soy protein isolate (SPI) complexes, thus improving their emulsifying properties. However, an excessive HIU treatment may lead to unfavourable unfolding of the protein structure, corresponding to the weakening of non-covalent forces [21,22]. Therefore, it is necessary to select the optimal HIU treatment power and duration to improve the emulsification performance of protein-polysaccharide complexes and the stability of lipophilic bioactive substances embedded in the emulsion. However, the effects of HIU treatment on the formation of CAS-HA complex emulsions and its application in the encapsulation of lipophilic bioactive substances have not been reported.

Herein, we prepared an emulsion stabilised by an ultrasound-treated CAS-HA complex and evaluated its bioavailability to deliver vitamin E into the gastrointestinal tract. This study aimed to enhance the emulsifying property of the CAS-HA complex by HIU treatment and effectively protect vitamin E during in *vitro* digestion. Meanwhile, to prevent the adverse effects of excessive HIU treatment, we compared the structure and emulsifying properties of CAS-HA complexes under different HIU powers (75, 150, and 300 W) and different durations (5, 10, and 20 min) to determine the most optimal HIU conditions. Finally, an emulsion stabilised by ultrasound-treated CAS-HA complex was designed as a novel delivery carrier to improve vitamin E bioavailability. This study provides a reference for innovative food emulsifiers to improve the delivery and encapsulation design of lipophilic bioactive substances.

2. Materials and method

2.1. Materials

Casein powder (80 % protein) was obtained from Sigma-Aldrich. Hyaluronic acid (194 kDa) was obtained from Focusfreda Biological Co., ltd. (Shandong, China). Vitamin E was purchased from Shanghai Yuanye Bio-Technology Co., ltd. (Shanghai, China). Other chemicals were of analytical grade.

2.2. Preparation of CAS-HA complexes

CAS solutions (3 %, w/v) were prepared with deionized water, then adjusted the final pH of the solution to 7.0 with 1.0 mol/L NaOH, and stored at 4 °C for 8 h. Subsequently, the CAS solutions were mixed with HA powder and stirred at 800 rpm for 2 h to dissolve it completely to obtain complex solutions with 0.5 % (w/v) HA concentration. All samples were obtained at 25 °C.

2.3. HIU treatment

The CAS and CAS-HA complexes were treated using a probe sonicator (JY92-IIDN, Ningbo Scientz Biotechnology Co., China). One hundred milliliters of the CAS-HA complex solutions were added to a beaker (inner diameter ≈ 7.3 cm, height ≈ 9.2 cm). The pulse working time was 2 s, the intermittent time was 2 s, and the ultrasonic titanium probe with a diameter of 6 mm was immersed in the CAS-HA complex solution at a depth of 1 cm from the bottom, followed by treatments with different output powers (75 W, 150 W, 300 W) and durations (5 min, 10 min, 20 min) at 20 kHz. During HIU treatment, the temperature of samples was controlled at 15 °C ± 1 °C with an ice-water bath. The prepared CAS-HA complex solution was lyophilized to powder by freeze dryer for further study. The final complexes contained eight groups and labeled in Table 1.

2.4. Characterization of CAS-HA complex solutions

2.4.1. Particle size and zeta potential

The solution for particle size determination was diluted to a protein concentration of 0.1 % (w/v) with ultrapure water. The particle size and zeta potential of the samples after dilution were determined by the dynamic light scattering (DLS) technique using a NANO ZS90 (Malvern Instruments ltd., UK) [23].

2.4.2. Intrinsic fluorescence

The fluorescence intensity was determined by a fluorescence spectrometer (F-7100, Hitachi Corporation, Japan). Diluted the sample with ultrapure water to a protein concentration of 0.1 % (w/v). The emission wavelength was collected from 300 nm to 450 nm and the slit widths and the excitation wavelength were set at 5 nm and 290 nm, respectively [23].

Table 1
CAS and CAS-HA complexes under different HIU treatments.

Samples	CAS (%, w/v)	HA (%, w/v)	HIU power (W)	HIU duration (min)
CAS	3	0	–	–
CAS-HA	3	0.5	–	–
U150-5	3	0.5	150	5
U150-10	3	0.5	150	10
U150-20	3	0.5	150	20
U75-10	3	0.5	75	10
U300-10	3	0.5	300	10

2.4.3. Surface hydrophobicity (H_0)

Four milliliters of the diluted sample (0.1 %, w/v) were mixed with 20 μL of ANS (8.0 mmol/L, pH 7.0) and scanned by a fluorescence spectrophotometer (F-7100, Hitachi Corp., Japan) to obtain the fluorescence spectra (excitation wavelength at 390 nm, emission wavelength from 400 to 600 nm, excitation and emission slits of 5 nm) [23].

2.4.4. Circular dichroism (CD)

Samples were diluted with ultrapure water to a protein concentration of 0.01 % (w/v). CD spectra were recorded in the far ultraviolet (190–260 nm) region using a Chirascan V100 spectropolarimeter (Applied Photophysics ltd., England) at room temperature using a 1.0 mm path length cell. Finally, the secondary structure score of the protein was calculated according to the CD website (https://dichroweb.cryst.bbk.ac.uk) [23].

2.4.5. Fourier transform infrared spectroscopy (FTIR)

The infrared spectra of the lyophilized powder were measured by infrared spectrometer (Nicolet iS10, Thermo Fisher Scientific, Germany). The spectra were recorded at an average of thirty-two scans from 600 to 4000 cm^{-1} at room temperature [23].

2.4.6. Creaming index (CI) and appearance of emulsions

The freshly emulsions stabilized by ultrasound-treated CAS-HA complex were added into glass bottles to store at room temperature for 14 d. Emulsion appearances were observed at 1 and 14 d, and CI were gained using the following Eq. [24].

$$CI(\%) = \frac{H_C}{H_E} \times 100$$

The H_C represents the height of cream layer; the H_E represents the total height of emulsions.

2.4.7. Emulsifying ability index (EAI) and emulsifying stability index (ESI)

EAI and ESI were determined using a turbidimetric method. The crude emulsion (80 μL) was taken immediately after preparation and 10 min later and diluted in 0.1 % sodium dodecyl sulfate (1:100, v/v). Absorbance at 500 nm of the mixture was detected using Uultraviolet (UV) spectrophotometer (T9, PUXI, China) [21]. EAI and ESI were expressed as:

$$EAI\left(m^2/g\right) = \frac{A_0 \times N}{(1-\varphi) \times C \times 10^4} \times 2T$$

$$ESI(min) = \frac{A_0 \times 10}{A_0 - A_{10}}$$

A_0 and A_{10} represent the absorbances of the measured solutions at 0 and 10 min, respectively; N represents the dilution factor; C is the protein concentration (g/mL); φ represents the oil volume fraction; and T is 2.303.

2.4.8. Percentage of adsorbed proteins (AP)

The aqueous phase of emulsions was obtained by centrifugation (13,000×g, 30 min) at room temperature. Afterwards, the aqueous phase was filtered using a 0.45 μm filter and the protein concentration was determined using a BCA Protein Assay Kit [25].

$$AP(\%) = \frac{C_0 \times C_s}{C_0} \times 100$$

where C_0 is initial protein concentration, C_s is concentration of protein in filtrate.

2.5. Preparation of emulsions

The soybean oil was used as the oil phase and the obtained CAS-HA complexes were used as the water phase. Next, vitamin E (10 % w/v with respect to the soybean oil) was fully dissolved in soybean oil. Emulsions were prepared with a controlled oil/water volume ratio of 20/80 and homogenized (IKA-T25, Germany) at 13,000 rpm for 2 min.

2.6. Characterization of CAS-HA emulsions

2.6.1. Confocal laser scanning microscopy (CLSM)

The microstructures of emulsions at 1 d and 14 d were obtained using a confocal laser scanning microscope (Deltavision OMX SR, USA). Nile blue (used to label proteins) and Nile red (used to label lipids) were excited by 488-nm Ar/Kr and 633-nm He/Ne lasers, respectively. The stained sample (5 μL) was dropped on a slide, carefully covered with a cover slide, and observed at a magnification of 60× [25].

2.6.2. Rheological property

Rheological behavior was analyzed with dynamic shear rheometer (MARS40, HAAKE, Germany) using a parallel plate (60 mm diameter, 1 mm gap) geometry probe at 25 °C. The strain was set as 1 % to avoid destruction of the emulsion network structure. The frequency sweep tests were conducted (0.1 Hz–10.0 Hz). The shear rate sweep tests were performed over a shear rate range of 0.1–100 s^{-1} to measure the apparent viscosity [25].

2.7. In vitro digestion

2.7.1. Simulated gastrointestinal tract (GIT) digestion

The digestive behaviors of emulsions and the bioaccessibility of vitamin E was evaluated using simulated gastrointestinal tract (GIT) model. The preparation of digestive fluids refers to previous study [1].

Gastric stage: Adjust the pH of simulated gastric fluid (SGF) containing 32 mg/mL pepsin to 1.2 with 1.0 mol/L HCl. Subsequently, the pH of the emulsion sample (10 mL) was adjusted to 2.0 using 0.1 mol/L HCl, and then mixed with SGF with continuous shaking at 37 ℃ for 120 min.

Intestinal stage: the pH of the solution was adjusted to 7.0 using 1.5 mol/L $NaHCO_3$ to inactivate pepsin. Emulsion sample (10 mL) was mixed with simulated intestinal fluid (SIF) containing 20 mg/mL bile salt, 10 mg/mL pancreatin, and 0.75 mol/L $CaCl_2$ at a ratio of 1:2 (v/v). Then shaked continuously for 120 min at 37 ℃. Finally, the sample was soaked in an ice bath for 10 min to stop the reaction.

2.7.2. Particle size and zeta potential

Particle size was tested at 25 ℃ using a Malvern 3000 laser diffraction particle sizer (Mastersizer 3000E, Malvern, England). Emulsions (1–3 mL) were placed in a sample tank and diluted automatically in the instrument, and the particle size was measured when the light blocking rate reached 10 % [26]. The zeta potential of emulsions was measured as described in section 2.4.1. The emulsion (100 μL) was diluted 50 times before testing.

2.7.3. Bioaccessibility

The sample (10 mL) after simulate intestinal digestion was removed and centrifuged at 4000 rpm for 40 min. The phase over the sediment represented the "micelle" fraction in which the vitamin E was dissolved. The micelle phase (1 mL) was mixed with the solvent (5 mL, ethanol: *n*-hexane (v/v, 1:2)), vortexed, and centrifuged for 5 min at 1000 rpm. The resulting samples were measured by ultraviolet (UV) spectrophotometer (T9, PUXI, China) at 285 nm. Vitamin E content was obtained from the Vitamin E standard curve ($y = 0.0045x + 0.0072$, $R^2 = 0.9995$). Bioaccessibility was then calculated using following equation [26]:

$$\text{Bioaccessibility} = \frac{C_{\text{Micelle}}}{C_{\text{Original Digesta}}} \times 100\%$$

where $C_{Original\ Digesta}$ and $C_{Micelle}$ are the Vitamin E concentrations in the original digestion and micelle fractions after the digestion experiment.

2.8. Statistical analysis

Data are presented as means ± standard deviation (SD) of three samples in each group. An analysis was carried out in SPSS 26.0 (SPSS, Inc., Chicago, IL, USA). Differences among groups have been assessed and analyzed in a one-way ANOVA and Duncan's multiple range test. According to the results, a value of $P < 0.05$ demonstrated a difference in statistics.

3. Results and discussion

3.1. Effect of HIU treatment on the CAS-HA complex solutions

3.1.1. Zeta potential and particle size

Fig. 1A shows the zeta potential of CAS and CAS-HA complex solutions under different HIU treatments. The zeta potential of CAS has been reported to be –35.4 mV at pH = 6.7 [27], which is similar to our result (–37.1 mV). The zeta potential of a single HA is –69.55 mV. When HA was added to CAS, the absolute potential of the CAS-HA complex increased significantly from 37.1 to 44.1 mV. Electrostatic repulsion occurred when both HA and CAS were negatively charged. Similarly, citrus pectin enhanced the electrostatic repulsion, thus improving the emulsion stability [21]. Although there is electrostatic repulsion between CAS and HA, there may still be positively charged patches on the surface of casein that interact with HA, leaving CAS and HA to form a soluble complex [28]. In general, soluble complexes formed between proteins and polysaccharides can form a protective layer at the oil–water interface, which can be beneficial in inhibiting the aggregation of oil droplets and, consequently, improving the stability of emulsions [29]. After HIU treatment, the absolute zeta potential of the U150-10 group was the highest, indicating that the electrostatic interaction of this group was the strongest. HIU treatment unfolds protein molecules and disrupts protein aggregation, thereby increasing the net charge on the protein surface [21].

The particle size distribution of the CAS and CAS-HA complexes under HIU treatment is shown in Fig. 1B. Naturally, all samples showed a multi-peak distribution. From Fig. 1C, the average size of CAS decreased significantly from 387.3 to 319 nm after HIU treatment, indicating that the shear force generated during the HIU treatment can reduce the particle size and destroy insoluble aggregates [21]. After the addition of HA, the average particle size of the solution decreased from 387.3 to 372.2 nm, while the PDI increased significantly from 0.4615 to 0.8013. This may be due to the formation of a soluble complex between CAS and HA [26]. During the HIU treatment, the shear force and turbulence caused by cavitation resulted in the dissociation of the large particles of the CAS-HA complex, and thus the particle size and PDI of the U150-10 group decreased significantly to 247.6 nm and 0.5669, respectively [30]. However, the higher power (300 W) or longer duration (20 min) of the HIU treatment increased the average particle size of the complex, which can be attributed to protein re-aggregation and formation of soluble protein-polysaccharide complex caused by excessive ultrasonication [21]. Apparently, different powers and durations have a significant impact on zeta potential and particle size.

3.1.2. Intrinsic fluorescence spectrum

Tryptophan (Trp) is sensitive to microenvironment polarity; therefore, Trp fluorescence analysis is often used to evaluate changes in protein structure [23]. Fig. 2A depicts the intrinsic fluorescence spectra of CAS and CAS-HA complexes under HIU treatment. CAS showed a maximum fluorescence wavelength (λ^{max}) at 352 nm, and HIU treatment led to an increase in fluorescence intensity. HIU treatment unfolds the protein structure, exposing tryptophan residues previously buried in the internal hydrophobic region of the protein [18]. Conversely, the Trp fluorophore of CAS is effectively quenched due to the steric effect of HA. Meanwhlie, HA caused a blue shift of λ^{max} from 352 to 350 nm, indicating that HA induces a conformational change of CAS, leading to a shift of Trp residues to a less polar environment [31]. Compared to CAS-HA, HIU treatment increased the fluorescence intensity of the solutions, which may be attributed to the non-covalent interaction between CAS and HA enhanced by HIU treatment; thus, more Trp residues are adsorbed on the polar surface [21]. The fluorescence intensity of the U150-10 group was the highest, indicating that HIU treatment unfolded the protein structure and exposed more Trp. Compared to the U150-10 group, the fluorescence intensity of the U300-10 and U150-20 groups decreased significantly, possibly because the cavitation effect caused by the formation and collapse of bubbles during the HIU treatment destroyed the protein structure, promoted hydrophobic interaction between molecules, and formed aggregates that buried the exposed amino acids [18].

3.1.3. Circular dichroism (CD) spectroscopy

The secondary structure of proteins is determined by Circular dichroism (CD) spectroscopy. From Fig. 2B, the CD spectrum of CAS showed a broad negative maximum at approximately 200 nm, suggesting that CAS is rich in random coil and β-sheet [32]. Specifically, the content of secondary structure is shown in Fig. 2C. Compared with CAS, the β-sheet content of CAS-HA decreased by 2.3 %, and the random coil and β-turn content of CAS-HA increased by 0.9 and 1.2 %, respectively. The attachment of carbohydrate chains changed the conformation of CAS, revealing the transformation of the protein structure from ordered to disordered [33]. As the HIU power increases from 75 to 150 W or the duration increases from 5 to 10 min, the content of β-sheet and α-helix decreases, while the content of random coil and β-turn increases. HIU treatment promotes hydrogen bond breaking of the stable protein structure, leads to loosening of the protein molecular structure, and reduces the content of ordered structures in CAS molecules [18,19].

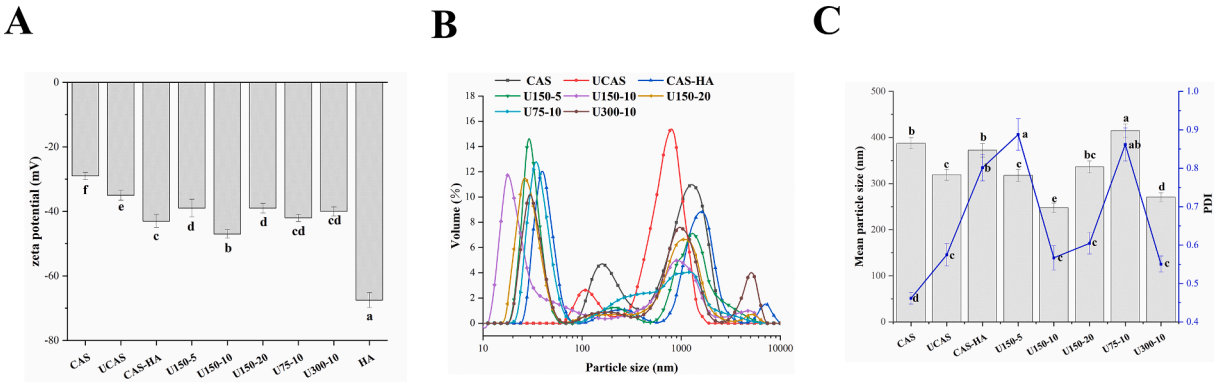

Fig. 1. Effect of HIU treatments on the zeta potential (A), particle size distribution (B), and mean particle size (C) of CAS and CAS-HA complexes. Different lowercase letters (a–f) indicate significant differences ($P < 0.05$) in the mean values within the same parameter group.

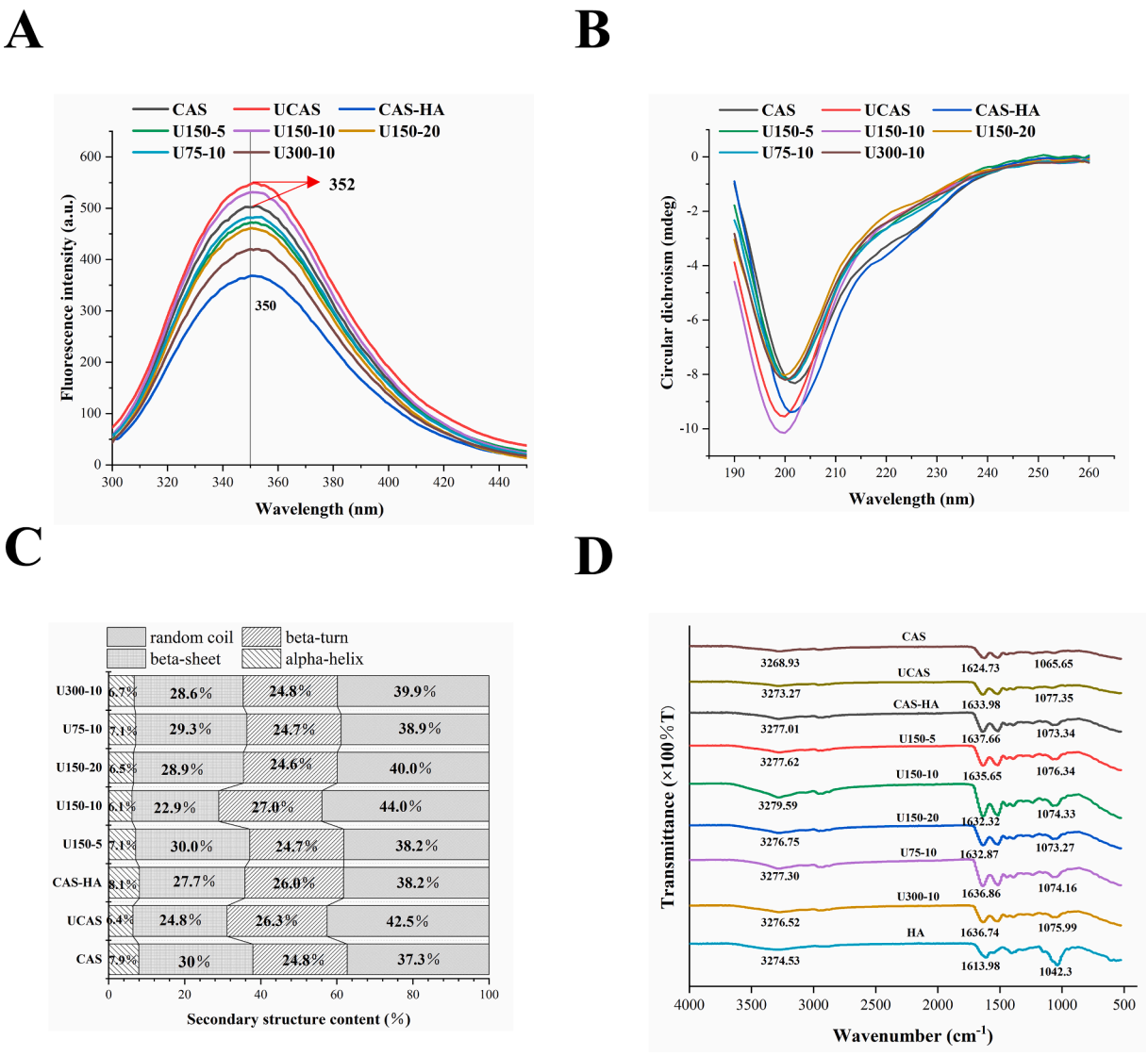

Fig. 2. Effect of HIU treatments on the fluorescence spectra (A), circular dichroism spectra (B, C), and FTIR spectroscopy (D) of CAS and CAS-HA complexes.

When the HIU power is further increased to 300 W or the duration is further extended to 20 min, the α-helix and β-sheet content increases significantly, while the β-turn and random coil content decreases. The excessive internal thermal effect induced by the HIU treatment leads to aggregation of the protein particles instead of remaining in the unfolded state, and their structure changes from disordered flexibility to ordered rigidity [29]. The same phenomenon was observed in soy protein isolate-pectin complexes [18]. The reduction in α-helix and β-sheet and the increase in random coil and β-turn lead to a higher flexibility of the CAS-HA complex structure compared to single CAS, indicating that the CAS-HA complex can be more effectively adsorbed on the surface of oil droplet [34].

3.1.4. Fourier transform infrared (FTIR) spectroscopy

FTIR spectroscopy could reveal the interactions between CAS and HA under HIU treatment [26]. As shown in Fig. 2D, for pure HA, the band at 3274.53 cm^{-1} corresponds to the stretching vibration of O—H; the bands at 1613.98 cm^{-1} were caused by the symmetric and asymmetric vibrations of –COO–, respectively; and finally, the band at 1042.3 cm^{-1} refers to the stretching vibration of C—O—C [13]. Characteristic CAS peaks in the amide A band (–OH stretching) and amide I band (C═O stretching) were observed at 3268.93 and 1624.73 cm^{-1}, respectively [26]. This is consistent with the result of CD spectroscopy. As an indication of hydrogen bonding (–OH stretching), the HIU treatment significantly shifted the –OH of CAS from 3268.93 to 3273.27 cm^{-1}. This phenomenon shows that HIU treatment cause an effect on the hydrogen bonding between CAS molecules [26]. In addition, the peak at 1000–1200 cm^{-1} is typically generated by the vibration of C—O—H or C—O—C [35]. When HA was added, the absorption peak of CAS-HA was significantly shifted from 1065.65 to 1073.34 cm^{-1}, and the peak intensity increased significantly, indicating that HA formed complexes with CAS and formed more C—O—C or C—O—H bonds [36]. Meanwhile, the addition of HA shifted the hydrogen bonding to a higher wave number, indicating the existence of hydrogen bonding between CAS and HA [36,37]. After the CAS-HA complex was treated with HIU treatment, the blue shift of the amide I band suggested that HIU treatment may result in the α-helical structure of the CAS-HA complex becoming an amorphous β-sheet structure [38]. Compared with CAS-HA, the –OH of the U150-10 group shifted from 3277.62 to 3279.59 cm^{-1}, indicating that HIU treatment affected the hydrogen bonding of CAS and HA [26]. Meanwhile, the highest hydrogen bonding peak was observed in the U150-10 group. This phenomenon was attributed to the modification of sulfhydryl groups after ultrasonic treatment, which increased the number of available hydrogen bond donors and acceptors [39]. Conversely, when the power or duration is continuously increased, the –OH of the U300-10 and U150-20 groups blue shifted to 3276.52 and 3276.75

cm^{-1}, respectively. This may be related to protein reaggregation and the reformation of intermolecular hydrogen bonds caused by HIU treatment [29,35]. These results indicated that HIU significantly affectd the hydrogen bonds between CAS and HA and the secondary structure of protein molecules.

3.1.5. Surface hydrophobicity (H_0)

As shown in Fig. 3A, HIU improved the H_0 of CAS. Similarly, HIU treatment increased the H_0 of cod protein and promoted its adsorption on the oil–water interface, thus preventing emulsion instability [19]. Conversely, the H_0 of CAS-HA was significantly lower than that of CAS. This phenomenon can be explained as: (i) the increased electrostatic repulsion and steric hindrance of HA changed the CAS conformation and the shielded the binding of hydrophobic amino acids to ANS probes [40]. (ii) HA introduced a lot of hydrophilic groups. In addition, the H_0 of CAS-HA exhibited an increasing and then decreasing trend with HIU power or duration. This indicates that the original protein structure is destroyed by the ultrasonic cavitation effect and the hydrophobic groups are exposed, which enhances the hydrophobic force between the food components [39]. However, H_0 decreased significantly when the HIU power was further increased to 300 W or the duration was increased to 20 min, which may be because the excessive HIU treatment over unfolded the protein, and many hydrophobic groups were reburied, which inhibited the hydrophobic interaction between the molecules and led to the decrease of H_0 [21].

3.1.6. Percentage of adsorbed proteins (AP)

The flocculation and aggregation stability of an emulsion is affected by the percentage of adsorbed proteins (AP) at the oil–water interface. The interface is completely covered with adsorbed proteins, which prevents aggregation and flocculation of the oil droplets [25]. As shown in Fig. 3B, the CAS-HA complex is more easily adsorbed at the oil–water interface than CAS. This can be attributed to the fact that HA enhances the electrostatic interaction and steric barrier between oil droplets. Additionally, AP first increased and then decreased with HIU power and duration. This is because the ultrasonic cavitation effect caused the partial unfolding of the protein, which increased the conformational flexibility and adsorption capacity of the CAS-HA complex interface [25]. AP decreased when the HIU power or duration was further increased to 300 W or 20 min, respectively, which may be due to the reaggregation of protein particles caused by excessive ultrasonic treatment, and the crowding of neighbouring molecules in the adsorbed layer, thus limiting further unfolding [20].

3.1.7. Emulsifying properties

Fig. 3C shows the emulsifying properties of the CAS and CAS-HA complexes under HIU treatment. EAI characterises the ability of the complex emulsifier to form an emulsion; ESI characterises the ability of the complex emulsifier to maintain the stability of the emulsion [41]. Zhang et al. [7] observed that HIU treatment improved the emulsifying properties of CAS, which was consistent with our results. HA significantly improved the emulsifying properties of CAS, which can be attributed to the fact that HA increased the adsorption rate of the interfacial protein of the CAS-HA complex, and the complexes on the oil droplet surface formed a viscoelastic membrane to inhibit the unstable separation phenomenon [41].

HIU treatment usually produces powerful cavitation to make the system more uniform, thus increasing the possibility of contact between CAS and HA molecules, which favours complex formation [21]. As the HIU power or duration increased from 0 to 150 W or 10 min, respectively, EAI and ESI gradually increased. As mentioned before, an appropriate HIU power could enhance the non-covalent interactions between protein and polysaccharide and thus enhance the emulsifying properties of the complex emulsifier [42]. However, a further increase in HIU power or duration led to a decrease in EAI and ESI. The physical and thermal effects caused by the excessive energy input disturbed the internal structure of CAS-HA, leading to the embedding of hydrophobic groups and the formation of large aggregates, which negatively affected its emulsifying properties [43]. Ma et al. [21] reported that excessive HIU treatment could reduce the emulsifying properties of soybean protein isolate (SPI)-citrus pectin (CP). The authors also suggested that excessive power would disrupt the conformation of SPI, leading to

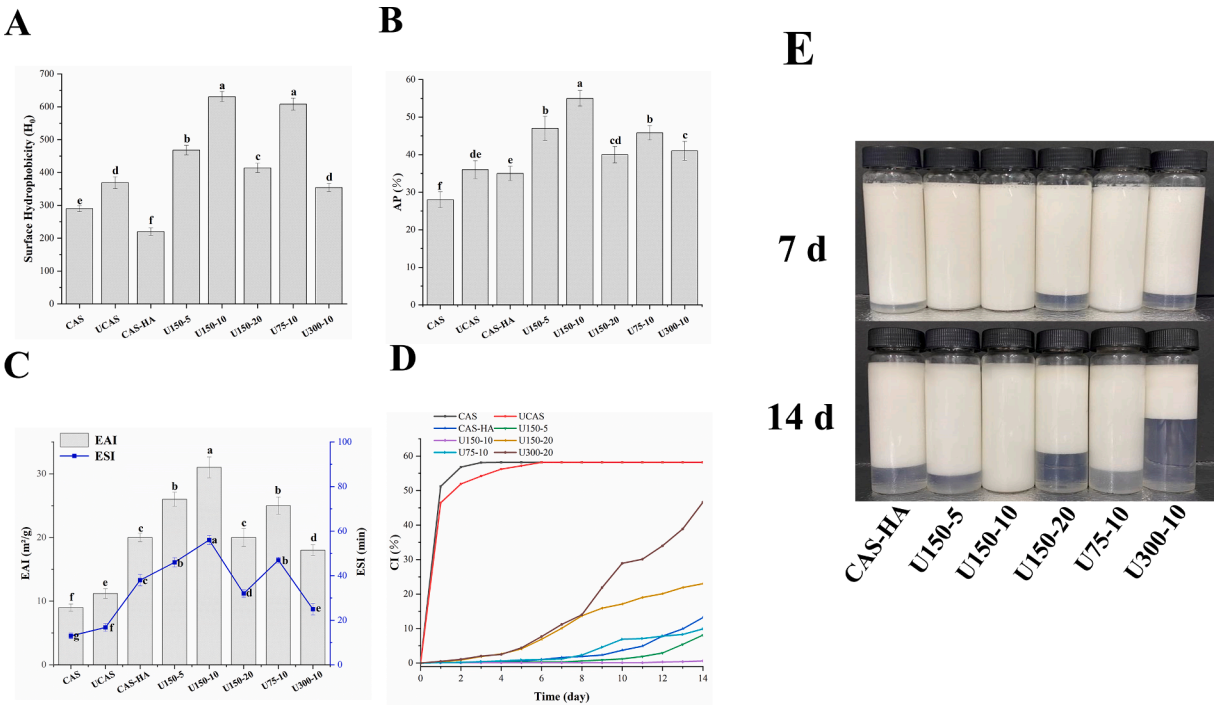

Fig. 3. Effect of HIU treatments on the surface hydrophobicity (H_0) (A), percentage of adsorbed proteins (AP) (B), EAI and ESI (C) of CAS and CAS-HA complexes. Creaming idex (CI) (D) and macroscopic appearance (E) of the emulsions stabilised by ultrasound-treated CAS-HA complex. Different lowercase letters (a–f) indicate significant differences ($P < 0.05$) in the mean values within the same parameter group.

reduced emulsifying properties.

3.1.8. Creaming index (CI)

The CI and morphologies of CAS-HA-stabilised emulsions under different HIU treatments are shown in Fig. 3D and 3E, respectively. CAS and UCAS show significant delamination after 1 h of storage. This may be due to the low concentration of CAS, which is not enough to cover the oil–water interface and form a stable interfacial film. HA significantly enhanced the stability of the CAS-stabilised emulsion. The treatment with HIU affects the hydrogen bonding and electrostatic interaction between proteins and polysaccharides, thus changing the molecular structure and morphology, which helps to form complexes with enhanced emulsifying properties. The CI of emulsions stabilised by the CAS-HA complex, U300-10 group, and U150-20 group increased significantly after 7 d, indicating that the stability of the emulsion decreased. This is because the excessive treatment with HIU does not favour the formation of a stable oil–water interfacial film [20]. After 14 d of storage, the emulsions of the U150-5 and U75-10 groups showed significant stratification. In contrast, the appearance of the emulsion stabilised by the U150-10 group hardly changed. The results showed that appropriate HIU treatment can help to form emulsifiers with a smaller particle size, which can be adsorbed on the droplets to form a dense interface layer. The dense interface layer provides sufficient steric hindrance for the emulsion to keep stable [41].

3.2. Effect of HIU treatment on the CAS-HA-stabilized emulsion

3.2.1. Rheological properties

The interaction between protein and polysaccharide at the interface will affect the viscoelasticity of the adsorption layer, thus having an impact on the stability of the formed emulsion. Generally, the storage modulus (G′) and loss modulus (G″) are used to evaluate the viscoelasticity of emulsion [41]. From Fig. 4A, the G′ of CAS and UCAS is low and changes irregularly, indicating that the emulsions stabilised by CAS and UCAS have a low and unstable network structure strength. This may be due to the large particle size of CAS and UCAS, which inhibits rapid adsorption at the oil–water interface, thus weakening their ability to form stable interfaces [44]. Notably, HA significantly increased the G' of the CAS-HA complex, which may reveal the improved emulsion network strength. This can be attributed to the fact that HA can form an entangled molecular network structure through intermolecular interaction, thus improving the strength of the emulsion network structure [45]. The G' of the emulsion stabilised by the CAS-HA complex under ultrasound treatment is further enhanced, and the maximum G' was observed in the emulsion stabilised by the U150-10 group, indicating that HIU treatments promoted the formation of a higher strength protein network structure, which can be attributed to the cavitation effect generated by ultrasound. This significantly changes the structure of the CAS-HA complex, promotes the interaction between the molecules adsorbed at the interface, and favours the formation of a network structure [35,39].

The precondition for the formation of a stable emulsion is not only limited to the interface G', but also the interface viscosity plays an important role in the emulsion stability. Generally speaking, the higher the emulsion viscosity, the more difficult the droplet movement, which favours emulsion stability [39]. From Fig. 4B, with increasing shear rate, the emulsion viscosity decreases significantly, which can be attributed to the fact that a higher shear rate can destroy the network structure of the emulsion, thus weakening the flow resistance [14,26]. HA, a type of macromolecular viscous polysaccharide, can affect the flow behaviour of the solution through strong hydration and chain entanglement effects [16]. Therefore, at a fixed shear rate, the viscosity of the CAS-HA complex is much higher than that of CAS, indicating a stronger interaction between molecules. In addition, the emulsion stabilised by the U150-10 group has the largest viscosity, which corresponds to the best emulsion stability.

3.2.2. Confocal laser scanning microscopy (CLSM)

The dispersion and size of the emulsion droplets were examined by CLSM. As shown in Fig. 4C, all micrographs showed that the droplets are oil-in-water structures. The average droplet size of CAS and UCAS is large and aggregated, indicating that the emulsification performance of CAS without HA is poor. Due to the strong electrostatic repulsion and

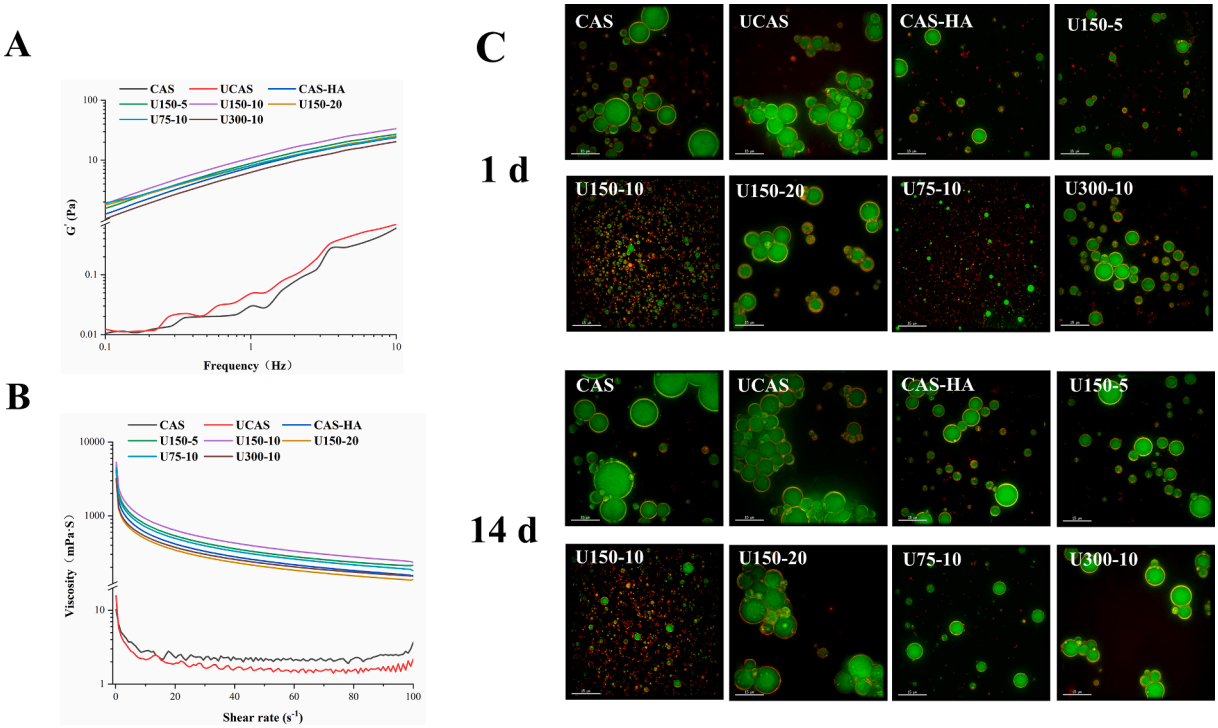

Fig. 4. Effect of HIU treatments on the storage modulus (G′) (A), apparent viscosity (B) and confocal laser scanning microscopy (CLSM) (C) of the emulsions stabilised by ultrasound-treated CAS-HA complex.

steric hindrance of HA, the droplet size of CAS-HA decreased significantly. The HIU-treated CAS-HA complex generates a more uniform emulsion, and the droplet size is further reduced and the distribution is more uniform. This may be because the proper ultrasonic cavitation can effectively disperse protein molecules aggregates, and the protein molecules can quickly adsorb on the oil–water interface, thus promoting the formation of small droplets [21]. However, the oil droplet size of the emulsions stabilised by the U300-10 and U150-20 groups increased and was not uniform, indicating that excessive HIU treatment will destroy the molecular structure of the CAS-HA complex, thus forming large particles and aggregates during emulsification [18]. After 14 d of storage, the average oil droplet size of all emulsions increased. Conversely, the droplet size of the emulsion stabilised by the U150-10 group increased slightly and maintained good homogeneity. The CLSM results are consistent with the emulsion storage morphologies.

3.3. *In vitro digestion of emulsions*

In *vitro* simulated digestion experiments were carried out to assess the digestion behaviours of the CAS-HA-stabilised emulsions. After incubation at each stage of the digestion process, the droplet size and zeta potential of the prepared emulsions were measured.

The particle size distribution of the initial emulsion is shown in Fig. 5A. The particle size of the emulsion stabilised by the U150-10 group is smaller than that of the CAS-HA group, which is consistent with the CLSM results. From Fig. 5B, the particle size of all emulsions has increased after passing through the gastric stage, suggesting that droplet aggregation occurred. Chen et al. [13] reported that the zein-HA binary complex was very aggregated in the gastric stage. Compared to the CAS-stabilised emulsion, a greater increase in particle size was observed in the CAS-HA complex-stabilised emulsions. This may be due to the formation of the electrostatic CAS-HA complex under the highly acidic conditions of the gastric stage [1]. Meanwhile, the pH conditions of the gastric stage could reduce the absolute value of the zeta potential and change the charge of all emulsions from negative to positive (Fig. 5D). These results suggested that the high acidic conditions in the stomach decreased the emulsion stability.

The particle size of the CAS-HA-stabilised emulsions incubated in the intestinal stage was much smaller than that of the emulsions incubated in the gastric stage. The decrease in particle size is due to the dissociation of the CAS-HA electrostatic complex caused by the change in pH value. Additionally, the high electrostatic repulsion between emulsion droplets in the intestinal stage makes them less prone to aggregation [4]. In addition, the size of all emulsions after simulated intestinal digestion was larger than their initial values. This may be because the absolute value of the zeta potential after the intestinal stage is smaller than that of the initial emulsion, which will result in the weakening of the electrostatic repulsion between the emulsion droplets [2].

The bioavailability of the lipophilic bioactive substance in the emulsion is one of the most important factors in the efficacy of a delivery vehicle. Fig. 5E showed the bioaccessibility of vitamin E in different emulsions after simulated gastrointestinal digestion. The bioaccessibility of vitamin E in the CAS-HA-stabilised emulsion (70.04 %) was significantly higher than that of the CAS-stabilised emulsion (43.56 %). This indicates that the incorporation of HA improves the protective capacity of the CAS-stabilised emulsion for vitamin E. HIU treatment further improved the bioaccessibility of vitamin E of the CAS-HA-stabilised emulsion to 79.64 %, suggesting that HIU treatment can further improve the protective capacity of the CAS-HA-stabilised emulsion for vitamin E in the simulated gastrointestinal tract digestion. This can be attributed to the reduced aggregation of the emulsion stabilised by ultrasound-treated CAS-HA complexes during digestion, whereby lipase more easily approaches oil droplets [46]. Consequently, the content of vitamin E released in the intestine increases.

4. Conclusion

In this work, we prepared an emulsion stabilised by ultrasound-treated CAS-HA complexes and used it to protect vitamin E during in vitro digestion. Results showed that HIU treatment affected the

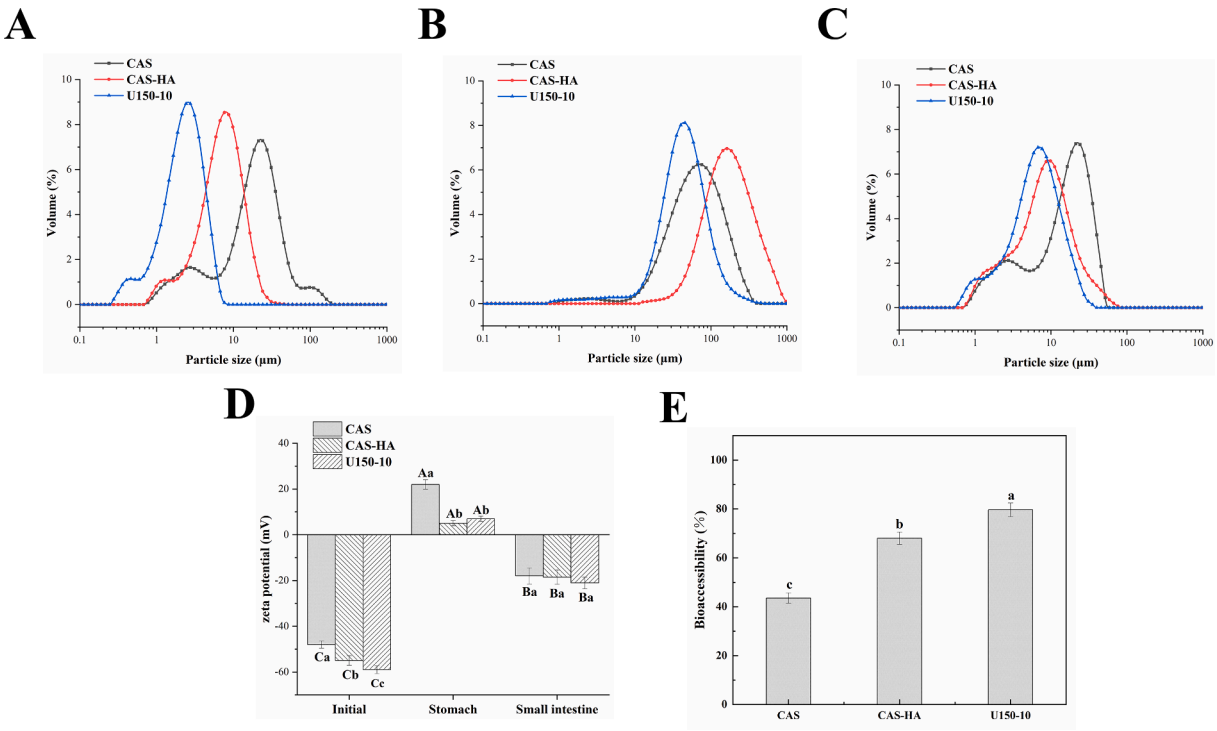

Fig. 5. Digestion characteristics of vitamin E-loaded emulsion stabilised by ultrasound-treated CAS-HA complex: particle size distribution of the original (A), gastric digestion (B), intestinal digestion (C) and zeta potential (D) for emulsion under different HIU treatments. Bioaccessibility (E) of vitamin E after digested in the simulated gastrointestinal tract. Different lowercase letters (a–c) indicate significant differences ($P < 0.05$) in the mean values within the same parameter group.

hydrogen bonding, electrostatic interaction and hydrophobic interaction between CAS and HA, leading to protein structure unfolding and an increase in the content of disordered structures. In addition, the HIU treatments increased the adsorption rate of the interfacial protein of the CAS-HA complex, thus improving its emulsifying properties. CLSM micrographs and storage results further demonstrated that the CAS-HA-stabilised emulsion showed the best stability after 14 d storage when treated at 150 W for 10 min. In *vitro* digestion experiments showed that the emulsion stabilised by the ultrasound-treated CAS-HA complex significantly improved the bioaccessibility of vitamin E from 43.56 to 79.64 % compared to the CAS-stabilised emulsion. This study may promote the preparation of more natural and stable emulsion delivery carriers that ensure the continuous or controlled release of lipophilic bioactive substances.

Declaration of Competing Interest

The authors declare that they have no known competing financial interests or personal relationships that could have appeared to influence the work reported in this paper.

Acknowledgements

The financial support for this project was provided by a special grant from Northeast Agricultural University. The program also was provided by postdoctoral program of Affiliated Hospital of Jining Medical University.

References

[1] X. Zhang, S. Zhang, M. Zhong, B. Qi, Y. Li, Soy and whey protein isolate mixture/calcium chloride thermally induced emulsion gels: Rheological properties and digestive characteristics, Food Chem. 380 (2022), 132212, https://doi.org/10.1016/j.foodchem.2022.132212.

[2] M. Zhong, F. Xie, S. Zhang, Y. Sun, B. Qi, Y. Li, Preparation and digestive characteristics of a novel soybean lipophilic protein-hydroxypropyl methylcellulose-calcium chloride thermosensitive emulsion gel, Food Hydrocoll. 106 (2020), 105891, https://doi.org/10.1016/j.foodhyd.2020.105891.

[3] C. Ma, S. Li, Y. Yin, W. Xu, T. Xue, Y. Wang, X. Liu, F. Liu, Preparation, characterization, formation mechanism and stability of allicin-loaded emulsion gel, LWT 161 (2022), 113389, https://doi.org/10.1016/j.lwt.2022.113389.

[4] G. Xu, C. Wang, P. Yao, Stable emulsion produced from casein and soy polysaccharide compacted complex for protection and oral delivery of curcumin, Food Hydrocoll. 71 (2017) 108–117, https://doi.org/10.1016/j.foodhyd.2017.05.010.

[5] G. Xu, L. Li, X. Bao, P. Yao, Curcumin, casein and soy polysaccharide ternary complex nanoparticles for enhanced dispersibility, stability and oral bioavailability of curcumin, Food Biosci. 35 (2020), 100569, https://doi.org/10.1016/j.fbio.2020.100569.

[6] C.S. Ranadheera, W.S. Liyanaarachchi, J. Chandrapala, M. Dissanayake, T. Vasiljevic, Utilizing unique properties of caseins and the casein micelle for delivery of sensitive food ingredients and bioactives, Trends Food Sci. Technol. 57 (2016) 178–187, https://doi.org/10.1016/j.tifs.2016.10.005.

[7] R. Zhang, X. Pang, J. Lu, L. Liu, S. Zhang, J. Lv, Effect of high intensity ultrasound pretreatment on functional and structural properties of micellar casein concentrates, Ultrason. Sonochem. 47 (2018) 10–16, https://doi.org/10.1016/j.ultsonch.2018.04.011.

[8] L. Liu, Q. Zhao, T. Liu, Z. Long, J. Kong, M. Zhao, Sodium caseinate/xanthan gum interactions in aqueous solution: Effect on protein adsorption at the oil–water interface, Food Hydrocoll. 27 (2) (2012) 339–346, https://doi.org/10.1016/j.foodhyd.2011.10.007.

[9] A.Q. Bi, X.B. Xu, Y. Guo, M. Du, C.P. Yu, C. Wu, Fabrication of flavour oil high internal phase emulsions by casein/pectin hybrid particles: 3D printing performance, Food Chem. 371 (2022), 131349, https://doi.org/10.1016/j.foodchem.2021.131349.

[10] Q. Zhao, Z. Long, J. Kong, T. Liu, D. Sun-Waterhouse, M. Zhao, Sodium caseinate/flaxseed gum interactions at oil–water interface: Effect on protein adsorption and functions in oil-in-water emulsion, Food Hydrocoll. 43 (2015) 137–145, https://doi.org/10.1016/j.foodhyd.2014.05.009.

[11] T. Zhang, R. Xu, N. Zhao, J. Xu, F. Liu, X. Wei, M. Fan, Rational design of lycopene emulsion-based nanofood for Lactobacillus plantarum to enhance the growth and flavor production, Food Hydrocoll. 127 (2022), 107518, https://doi.org/10.1016/j.foodhyd.2022.107518.

[12] A. Mora-Gutierrez, R. Attaie, M.N. de González, Y. Jung, S. Woldesenbet, S. A. Marquez, Complexes of lutein with bovine and caprine caseins and their impact on lutein chemical stability in emulsion systems: Effect of arabinogalactan, J. Dairy Sci. 101 (1) (2018) 18–27, https://doi.org/10.3168/jds.2017-13105.

[13] S. Chen, Y. Han, Y. Wang, X. Yang, C. Sun, L. Mao, Y. Gao, Zein-hyaluronic acid binary complex as a delivery vehicle of quercetagetin: Fabrication, structural characterization, physicochemical stability and in vitro release property, Food Chem. 276 (2019) 322–332, https://doi.org/10.1016/j.foodchem.2018.10.034.

[14] S.G. Sutariya, P. Salunke, Effect of hyaluronic acid on milk properties: Rheology, protein stability, acid and rennet gelation properties, Food Hydrocoll. 131 (2022), 107740, https://doi.org/10.1016/j.foodhyd.2022.107740.

[15] A. Aguilera-Garrido, T. del Castillo-Santaella, F. Galisteo-González, M.J. Gálvez-Ruiz, J. Maldonado-Valderrama, Investigating the role of hyaluronic acid in improving curcumin bioaccessibility from nanoemulsions, Food Chem. 351 (2021), 129301, https://doi.org/10.1016/j.foodchem.2021.129301.

[16] W. Zhong, C. Li, M. Diao, M. Yan, C. Wang, T. Zhang, Characterization of interactions between whey protein isolate and hyaluronic acid in aqueous solution: effects of pH and mixing ratio, Colloids Surf. B Biointerfaces 203 (2021), 111758, https://doi.org/10.1016/j.colsurfb.2021.111758.

[17] W. Zhong, T. Zhang, C. Dong, J. Li, J. Dai, C. Wang, Effect of sodium chloride on formation and structure of whey protein isolate/hyaluronic acid complex and its ability to loading curcumin, Colloids Surf. A Physicochem. Eng. Asp. 632 (2022), 127828, https://doi.org/10.1016/j.colsurfa.2021.127828.

[18] N. Wang, X. Zhou, W. Wang, L. Wang, L. Jiang, T. Liu, D. Yu, Effect of high intensity ultrasound on the structure and solubility of soy protein isolate-pectin complex, Ultrason. Sonochem. 80 (2021), 105808, https://doi.org/10.1016/j.ultsonch.2021.105808.

[19] W. Ma, J. Wang, X. Xu, L. Qin, C. Wu, M. Du, Ultrasound treatment improved the physicochemical characteristics of cod protein and enhanced the stability of oil-in-water emulsion, Food Res. Int. 121 (2019) 247–256, https://doi.org/10.1016/j.foodres.2019.03.024.

[20] K.M. Albano, V.R. Nicoletti, Ultrasound impact on whey protein concentrate-pectin complexes and in the O/W emulsions with low oil soybean content stabilization, Ultrason. Sonochem. 41 (2018) 562–571, https://doi.org/10.1016/j.ultsonch.2017.10.018.

[21] X. Ma, T. Yan, F. Hou, W. Chen, S. Miao, D. Liu, Formation of soy protein isolate (SPI)-citrus pectin (CP) electrostatic complexes under a high-intensity ultrasonic field: Linking the enhanced emulsifying properties to physicochemical and structural properties, Ultrason. Sonochem. 59 (2019), 104748, https://doi.org/10.1016/j.ultsonch.2019.104748.

[22] Y. Ding, H. Ma, K. Wang, S.R. Azam, Y. Wang, J. Zhou, W. Qu, Ultrasound frequency effect on soybean protein: Acoustic field simulation, extraction rate and structure, LWT 145 (2021), 111320, https://doi.org/10.1016/j.lwt.2021.111320.

[23] Q. Liu, Y. Sun, J. Cheng, M. Guo, Development of whey protein nanoparticles as carriers to deliver soy isoflavones, LWT 155 (2022), 112953, https://doi.org/10.1016/j.lwt.2021.112953.

[24] P. Chen, B.Q. Yang, R.M. Wang, B.C. Xu, B. Zhang, Regulate the interfacial characteristic of emulsions by casein/butyrylated dextrin nanoparticles and chitosan based on ultrasound-assisted homogenization: Fabrication and characterization, Food Hydrocoll. 133 (2022), 107983, https://doi.org/10.1016/j.foodhyd.2022.107983.

[25] N. Wang, X. Zhao, Y. Jiang, Q. Ban, X. Wang, Enhancing the stability of oil-in-water emulsions by non-covalent interaction between whey protein isolate and hyaluronic acid, Int. J. Biol. Macromol. 225 (2022) 1085–1095, https://doi.org/10.1016/j.ijbiomac.2022.11.170.

[26] S. Wang, J. Yang, G. Shao, J. Liu, J. Wang, L. Yang, J. Li, H. Liu, D. Zhu, Y. Li, L. Jiang, pH-induced conformational changes and interfacial dilatational rheology of soy protein isolated/soy hull polysaccharide complex and its effects on emulsion stabilization, Food Hydrocoll. 109 (2020) 106075.

[27] N.X. Sun, Y. Liang, B. Yu, C.P. Tan, B. Cui, Interaction of starch and casein, Food Hydrocoll. 60 (2016) 572–579, https://doi.org/10.1016/j.foodhyd.2016.04.029.

[28] L. Ding, Y. Huang, X. Cai, S. Wang, Impact of pH, ionic strength and chitosan charge density on chitosan/casein complexation and phase behavior, Carbohydr. Polym. 208 (2019) 133–141, https://doi.org/10.1016/j.carbpol.2018.12.015.

[29] Y. Xiong, Q. Li, S. Miao, Y. Zhang, B. Zheng, L. Zhang, Effect of ultrasound on physicochemical properties of emulsion stabilized by fish myofibrillar protein and xanthan gum, Innov. Food Sci. Emerg. Technol. 54 (2019) 225–234, https://doi.org/10.1016/j.ifset.2019.04.013.

[30] Y. Zhang, S. Zhang, B.o. Song, X. Wang, W. Zhang, W. Li, X. Pang, H. Zhu, J. Lu, J. Lv, Multi-dimensional analysis of rennet-induced micellar casein gels after ultrasound, Int. Dairy J. 126 (2022) 105293.

[31] C. Ren, W. Xiong, D. Peng, Y. He, P. Zhou, J. Li, B. Li, Effects of thermal sterilization on soy protein isolate/polyphenol complexes: Aspects of structure, in vitro digestibility and antioxidant activity, Food Res. Int. 112 (2018) 284–290, https://doi.org/10.1016/j.foodres.2018.06.034.

[32] B. Tirgarian, J. Farmani, R. Farahmandfar, J.M. Milani, F. Van Bockstaele, Ultra-stable high internal phase emulsions stabilized by protein-anionic polysaccharide Maillard conjugates, Food Chem. 393 (2022) 133427.

[33] Y. Wei, C. Li, L. Zhang, L. Dai, S. Yang, J. Liu, L. Mao, F. Yuan, Y. Gao, Influence of calcium ions on the stability, microstructure and in vitro digestion fate of zein-propylene glycol alginate-tea saponin ternary complex particles for the delivery of resveratrol, Food Hydrocoll. 106 (2020) 105886.

[34] Z. Li, J. Xi, H. Chen, W. Chen, W. Chen, Q. Zhong, M. Zhang, Effect of glycosylation with apple pectin, citrus pectin, mango pectin and sugar beet pectin on the physicochemical, interfacial and emulsifying properties of coconut protein isolate, Food Res. Int. 156 (2022) 111363.

[35] S. Wang, H. Zhao, D. Qu, L. Yang, L. Zhu, H. Song, H. Liu, Destruction of hydrogen bonding and electrostatic interaction in soy hull polysaccharide: Effect on emulsion stability, Food Hydrocoll. 124 (2022), 107304, https://doi.org/10.1016/j.foodhyd.2021.107304.

[36] Y. Chen, Z. Li, X. Yi, H. Kuang, B. Ding, W. Sun, Y. Luo, Influence of carboxymethylcellulose on the interaction between ovalbumin and tannic acid via noncovalent bonds and its effects on emulsifying properties, LWT 118 (2020), 108778, https://doi.org/10.1016/j.lwt.2019.108778.
[37] T. Luan, L. Wu, H. Zhang, Y. Wang, A study on the nature of intermolecular links in the cryotropic weak gels of hyaluronan, Carbohydr. Polym. 87 (3) (2012) 2076–2085, https://doi.org/10.1016/j.carbpol.2011.10.029.
[38] Y. Ni, J. Li, L. Fan, Effects of ultrasonic conditions on the interfacial property and emulsifying property of cellulose nanoparticles from ginkgo seed shells, Ultrason. Sonochem. 70 (2021), 105335, https://doi.org/10.1016/j.ultsonch.2020.105335.
[39] J. Chen, X. Chen, G. Zhou, X. Xu, Ultrasound: A reliable method for regulating food component interactions in protein-based food matrices, Trends Food Sci. Technol. 128 (2022) 316–330.
[40] T. Moschakis, B.S. Murray, E. Dickinson, Microstructural evolution of viscoelastic emulsions stabilised by sodium caseinate and xanthan gum, J. Colloid Interface Sci. 284 (2) (2005) 714–728, https://doi.org/10.1016/j.jcis.2004.10.036.
[41] N. Zhao, H. Zou, S. Sun, C. Yu, The interaction between sodium alginate and myofibrillar proteins: The rheological and emulsifying properties of their mixture, Int. J. Biol. Macromol. 161 (2020) 1545–1551, https://doi.org/10.1016/j.ijbiomac.2020.08.025.
[42] A. Amiri, P. Sharifian, N. Morakabati, A. Mousakhani-Ganjeh, M. Mirtaheri, A. Nilghaz, Y.-G. Guo, A. Pratap-Singh, Modification of functional, rheological and structural characteristics of myofibrillar proteins by high-intensity ultrasonic and papain treatment, Innov. Food Sci. Emerg. Technol. 72 (2021) 102748.
[43] L. Huang, X. Ding, Y. Li, H. Ma, The aggregation, structures and emulsifying properties of soybean protein isolate induced by ultrasound and acid, Food Chem. 279 (2019) 114–119, https://doi.org/10.1016/j.foodchem.2018.11.147.
[44] Z. Liu, D. Lin, R. Shen, X. Yang, Bacterial cellulose nanofibers improved the emulsifying capacity of soy protein isolate as a stabilizer for pickering high internal-phase emulsions, Food Hydrocoll. 112 (2021), 106279, https://doi.org/10.1016/j.foodhyd.2020.106279.
[45] P. Hájovská, M. Chytil, M. Kalina, Rheological study of albumin and hyaluronan-albumin hydrogels: Effect of concentration, ionic strength, pH and molecular weight, Int. J. Biol. Macromol. 161 (2020) 738–745, https://doi.org/10.1016/j.ijbiomac.2020.06.063.
[46] X. Zhang, X. Chen, Y. Gong, Z. Li, Y. Guo, D. Yu, M. Pan, Emulsion gels stabilized by soybean protein isolate and pectin: Effects of high intensity ultrasound on the gel properties, stability and β-carotene digestive characteristics, Ultrason. Sonochem. 79 (2021), 105756, https://doi.org/10.1016/j.ultsonch.2021.105756.